Available online at www.sciencedirect.com
SCIENCE DIRECT®
Composites: Part A 34 (2003) 635–647
composites
Part A: applied science and manufacturing
www.elsevier.com/locate/compositesa

Effect of the manufacturing process on the interfacial properties and structural performance of multi-functional composite structures

S. Mahdi[a], B.A. Gama[a,b], S. Yarlagadda[a], J.W. Gillespie Jr.[a,b,c,*]

[a]*Center for Composite Materials, University of Delaware, 201 Composites Manufacturing Laboratory, Newark, DE 19716-3144, USA*
[b]*Department of Materials Science and Engineering, University of Delaware, Newark, DE 19716, USA*
[c]*Department of Civil and Environmental Engineering, University of Delaware, Newark, DE 19716, USA*

Received 30 August 2002; revised 15 January 2003; accepted 7 March 2003

Abstract

A composite integral armor (CIA) structure consists of various layers such as ceramics, rubber and polymer composites assembled in a precise sequence to provide superior ballistic and structural performance at low areal density. CIA structures were originally manufactured in a labor-intensive multi-step process. In recent years, vacuum-assisted resin transfer molding (VARTM) has emerged as an affordable manufacturing method for CIA structures. In this paper, the relationship between the manufacturing processes (i.e. VARTM and multi-step) and the mechanical performance of CIA beams is investigated by four-point bend tests. The behavior of the CIA is found to be highly dependent on the mechanism of stress transfer between the layers and the structures are found to fail progressively and provide significant ductility and capacity. The VARTM process is found to produce structures with superior mechanical performance. Moreover, the level of interface adhesion achieved during processing is shown to control the structural behavior of the CIA. Consequently, the Mode I fracture testing of VARTM and multi-step manufactured double-cantilever beams, representative of one interface of the CIA, is characterized. The resistance to crack growth of the specimens is also related to the manufacturing process, with the VARTM specimens achieving the highest fracture toughness.

Keywords: A. Layered structures; B. Strength; D. Mechanical testing; E. Injection moulding

1. Introduction

The US Army requires the development of lightweight ground vehicle structures that must satisfy structural (i.e. stiffness, strength, damage tolerance, fatigue and environmental durability) and ballistic performance at minimum weight. This need has led to the development of lightweight ceramic-faced composite integral armors (CIA) [1–4]. A CIA structure was initially developed by United Defense (USA), as part of the Composite Armored Vehicle Advanced Technology Demonstrator program. The CIA considered in the present work consists of a polymer composite cover layer, a layer of alumina ceramic tile, a layer of rubber and a polymer composite backing plate, as shown in Fig. 1.

CIA structures have traditionally been fabricated from a multi-step process involving a hand lay-up and fiber placement of the material layers and a vacuum bag cure of the structure. An epoxy adhesive material was used to consolidate the layers. More recently, however, specialized fabrication methods have been proven successful at manufacturing high quality complex composite parts. Vacuum-assisted resin transfer molding (VARTM) has been shown to provide significant cost savings compared to hand lay-up and fiber-placement processes [5], and it has been used to successfully fabricate CIA panels, ramps and hull structures [6], in a single-step process. A fully automated VARTM process has also been recently developed that incorporates sensors, actuators and advanced control systems [7–9].

The ballistic performance of CIA has been studied extensively. Moreover, the mechanics of deformation and

* Corresponding author. Address: Center for Composite Materials, University of Delaware, 201 Composites Manufacturing Laboratory, Newark, DE 19716-3144, USA. Tel.: +1-302-831-8149; fax: +1-302-831-8525.
E-mail address: gillespie@ccm.udel.edu (J.W. Gillespie Jr.).

1359-835X/03/$ - see front matter © 2003 Elsevier Science Ltd. All rights reserved.
doi:10.1016/S1359-835X(03)00091-5

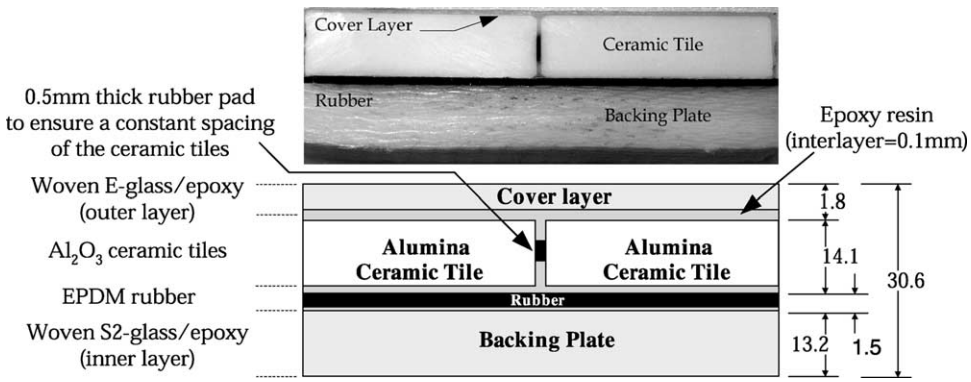

Fig. 1. Example of CIA (dimensions in mm are not to scale).

damage of particular layers has also been addressed extensively. Huang et al. [10] studied the mechanism of stress transfer between the ceramic tiles and the outer layer. Monib and Gillespie [11] and DeLuca et al. [12] investigated the ballistic performance of the S2-glass composite backing Plate. The failure mechanism of the ceramic tiles has been addressed experimentally [13] as well as numerically [14]. Gama et al. [4], Martinez et al. [15] and Zaera et al. [16] discussed the effect of a soft interlayer between the ceramic face and the backing plate on the ballistic performance of the armors. Also, analytical and numerical models were developed to predict the structural and ballistic behavior of such multi-layered structures [17–22].

However, the structural performance, damage tolerance and repair of CIA require further study before CIA hull structures can be fielded. The aim of the present work is to compare the structural performance of CIA beams manufactured by the VARTM process in a single-step operation, with that of CIA beams manufactured by the conventional multi-step process. It will be shown that the two processes lead to structures that are geometrically identical, but with material layer's interfacial properties that are fundamentally different. Consequently, the effect of the manufacturing process on the interface strength of the backing plate and the rubber layer is also investigated in this paper. The CIA beams are tested in a four-point bending test. The structural performance of single-step manufactured CIA is first described. The structural performance of multi-step CIA is then compared with that of the single-step CIA. A discussion on the effect of the surface mechanical preparation (mechanical abrasion) of the rubber layer to the structural performance of the CIA is also presented. Finally, the effect of the manufacturing process on the level of interface adhesion achieved between the backing plate and the rubber layer interface is assessed in a Mode I fracture mechanics test.

2. Manufacture

CIA structures were manufactured at the University of Delaware Center for Composite Materials (UD-CCM). The backing plate consisted of 22 layers of Vetrotex plain weave S2-glass fabric of areal weight 0.81 kg/m^2. The lay-up used was [0/90] (i.e. the fabric warp direction is at 0° and the weft direction is at 90°). The total thickness of the backing plate after impregnation with a tough epoxy resin was about 13.2 mm at a volume fraction of about 50%.

The rubber layer was 1.5 mm thick made of EPDM rubber (Ethylene Propylene rubber, Shore A 60). After being cut to the desired size, holes 6 mm in diameter, spaced by 50 mm, starting 25 mm from the edge of the layer were punched though the thickness of the rubber. The holes provided channels for resin and hence enhanced the bonding with the surrounding layers. The rubber surface was abraded on both sides using a rotary surface grinder with an alumina disc. The rubber was subsequently coated with a primer from Lord Corporation. The effect of rubber surface abrasion on the structural performance of the CIA was investigated by preparing beams in which the surface of the rubber was and was not mechanically abraded.

The alumina hexagonal ceramic tiles (AD-99.5) used were 142 mm long, 101.6 mm wide for a thickness of 14.1 mm. The tiles were degreased with acetone prior to manufacturing. A 0.5 mm thick soft rubber pad was placed between the tiles to ensure a constant spacing during and after the manufacturing operations. Fig. 2(a) shows a geometric configuration of ceramic tiles. To facilitate for an evaluation of the mechanical performance, the size of the test pieces is reduced to the size of a beam, 889 mm long by 101.6 mm wide, as shown in Fig. 2(b).

The cover layer consisted of five layers of Vetrotex twill weave 7781 E-glass fabric, also impregnated with an epoxy resin. The total areal-density achieved is about 86.6 kg/m^2. The mechanical properties of the materials used are presented in Table 1.

In the single-step and the multi-step manufacturing processes, the stack is consolidated with a toughened epoxy resin system, namely the Applied Poleramic SC15 epoxy resin system. The SC15 system gels overnight at room temperature and under vacuum. Additionally, a four-hour post-cure at 149 °C is done. In the multi-step manufacturing process [22], a more compliant Applied Poleramic SC11 epoxy resin system was also examined. The SC11 system is

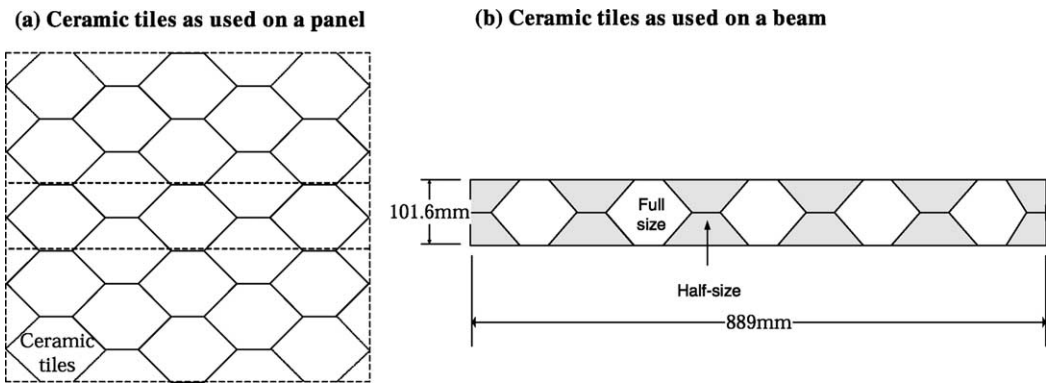

Fig. 2. Arrangement of ceramic tiles (a) a CIA panel and (b) a CIA beam.

a tough, almost rubbery, epoxy resin system. The SC11 system was cured at 121 °C for 2 h and was post-cured at 149 °C for another 2 h, under vacuum.

2.1. Single-step, vacuum assisted resin transfer molding, process for CIA beams

In the VARTM process, the entire CIA is made in one single operation in which resin is injected with the assistance of vacuum. A flat steel plate, cleaned and coated with release agent (Freekote), is used as a mold. First, five layers of the E-glass that constitutes the cover layer are placed down inside a wood frame as deep as the thickness of the CIA to be made. To provide for a thin interlayer between the cover layer and the ceramic tiles, a scrim cloth (one layer of 0.1 mm thick Vetrotex 1659 E-glass mesh) is placed over the stack of E-glass fabrics. The ceramic tiles are then laid down and arranged as shown in Fig. 2(b). The arrangement is such that there is a full-size tile at the center of the beams, followed by an arrangement of half-size and full-size tiles. Another layer of scrim cloth is next placed in the mold, followed by the rubber layer. The scrim cloth provides a controlled bond line thickness between the ceramic tiles and the rubber, as well as a path for the resin flow during infusion. Additionally, the holes produced in the rubber layer created an interconnected channel of resin between the two layers. The 22 layers of S2-glass are finally stacked in the mould. The assembly is then covered with peel ply and a resin distribution media. The resin inlet (a plastic omega channel) is placed in the middle of the stack and two vacuum lines are placed on breather cloth, outside the frame. A vacuum bag is next applied and the edges are sealed with a tacky tape. Vacuum is applied to the bag through a vacuum gauge mounted resin trap. The resin is then infused in the part through the resin inlet. It is noted, that in order to minimize resin circulation and waste, a micro-flow vacuum control (MIVACON) process, which has been developed at UD-CCM [7], was used. The lay-up arrangement of the process is shown schematically in Fig. 3. After the stack is completely infiltrated with SC15 resin, the resin inflow is stopped and the stack is ready for cure.

2.2. Multi-step process for CIA beams

The material layers used in the multi-step manufacturing process are identical to those used in the single-step

Table 1
Mechanical properties of the materials used (1, 2 and 3 are the longitudinal, transverse and though-thickness directions, respectively).

	Backing plate[a]	Rubber[a]	Ceramic[b]	Cover layer[a]	Epoxy SC15[c]	Epoxy SC11[c]
E_{11} (GPa)	27.5	3.5×10^{-3}	270	25.9	2.7	0.85
E_{22} (GPa)	27.5	3.5×10^{-3}	270	25.9	2.7	0.85
E_{33} (GPa)	13.7[b]	3.5×10^{-3}	270	13.7[b]	2.7	0.85
G_{12} (GPa)	2.85			2.85		
G_{13} (GPa)	3.26			3.26[b]		
G_{23} (GPa)	3.26[b]			3.26[b]		
ν_{12}	0.1084	0.49[b]	0.22	0.1084	0.37	0.37
ν_{23}	0.46[b]	0.49[b]	0.22	0.39[b]	0.37	0.37
ν_{13}	0.46[b]	0.49[b]	0.22	0.39[b]	0.37	0.37

[a] *From standard mechanical tests performed at UD-CCM.*
[b] *Estimated properties.*
[c] *Properties communicated by Applied Poleramic, CA, USA.*

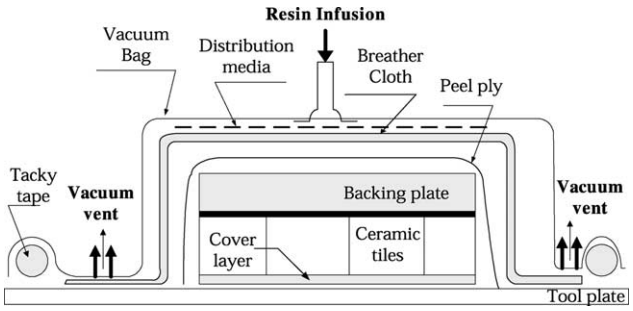

Fig. 3. Manufacture of CIA beams by the VARTM process.

manufacturing process. The various layers, however, are prepared individually and then joined together in a vacuum bag. The interfaces between all the layers are hand impregnated with either SC15 or SC11 resins.

The backing plate is fabricated first by the MIVACOM process [7] using the SC15 epoxy resin system, as described above. After injection and cure, the plate is cut to dimension, and its surface sandblasted and cleaned. The CIA is then assembled, in a second operation, to form the lay-up arrangement shown in Fig. 3. The five plies that constitute the cover layer are laid down, one at a time, in a wooden frame over a prepared mould surface, and are hand-impregnated by resin, which is spread out with a spatula. A layer of scrim cloth is then placed over the impregnated plies. The ceramic tiles are then placed over the stack that is saturated with resin. The other layer of scrim cloth, the rubber layer and the cured backing plate are finally placed in the mold, taking care that the all the interfaces are impregnated and saturated with resin. When the procedure is completed, the part is placed in a vacuum bag in order to compact the layers, and remove excess resin and air. The stack is then ready for cure of the resin systems.

3. Experimental

3.1. Four-point bend testing of CIA

The beams were tested statically in four-point bending as shown schematically in Fig. 4. The tests were conducted so that the cover layer is subjected to compression forces and the backing plate is subjected to tensile forces. The CIA beams were tested in an INSTRON 8562 machine. MEME CEA-06-500UW-350 strain gages, with a 15 mm gage length, were used for the determination of surface strains. The sequence of failure events was visually observed and noted as the displacement was increased at a constant rate of 2.5 mm/min, and as the load–displacement curve was recorded on a data acquisition system. Several beam configurations, described in Section 2, were tested:

Single-step SC15 VARTM process; impregnated with SC15 resin.

Multi-step SC15 The backing plate and the final consolidation are made with SC15 resin.

Multi-step SC11 The backing plate is fabricated with SC15 resin; the final consolidation is then made with SC11 resin.

In addition, the basic configurations described above are tested with and without a mechanical surface preparation (abrasion) of the rubber layer. Four single-step SC15 (SS-SC15) CIA beams were tested to allow for an analysis of the reproducibly of the results. The reproducibility in the results was found to be very good (as will be shown later) and subsequent configurations required only two replicates.

3.2. The effect of the manufacturing process on the backing plate/rubber interface toughness

In addition to the mechanical testing of the CIA beams, the effect of the manufacturing process on the interfacial toughness between the rubber layer and the backing plate is assessed by fracture mechanics experiments. Double cantilever beam (DCB) specimens, made of a layer of rubber sandwiched between two S2-glass/SC15 arms, representative of the interface between the backing plate and the rubber in the CIA beams, were manufactured by the single-step and multi-step processes. The specimens, with the dimensions as shown in Fig. 5, were cut from a sandwich plate that contained a 10 μm thick Kapton film at one end to simulate a starter crack.

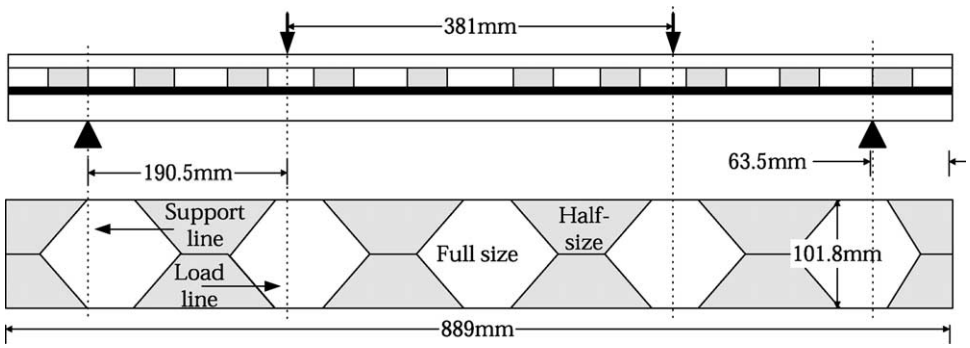

Fig. 4. A CIA panel in four-point bending.

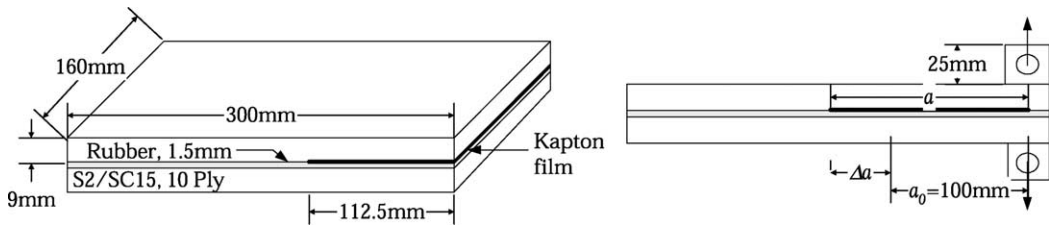

Fig. 5. Mode I fracture DCB specimens.

The single-step DCB coupons were fabricated in one operation in much the same way as the single-step CIA beams were fabricated (see Section 2.1). The 10 plies of S2-glass fabric that constitutes the first arm of the DCB specimens were laid down on the steel tool plate, followed by the rubber layer. The Kapton film was then carefully positioned at one end of the laminate. The second set of 10 ply of S2-glass fabric that constitutes the second arm of the DCB specimens were then positioned over the stack. The stack was finally bagged and impregnated by SC15 resin, as shown in Fig. 3.

The multi-step DCB coupons were fabricated in two operations similar to the multi-step CIA beams (see Section 2.2). First, a 10 ply S2-glass/epoxy plate was fabricated by the VARTM process, and impregnated with SC15 resin. The plate constituted the materials for the two arms of the DCB. The plate was grit blasted, cleaned and cut to the dimensions as shown in Fig. 5. The sandwich stack was then manufactured in a second operation, by hand impregnation of the SC15 or SC11 resins. A set of multi-step DCB specimens was also manufactured in which the rubber layer was not abraded.

Five specimens, 25 mm wide, were cut from each plate. Aluminum end blocks (25 mm by 25 mm) were then bonded at the delaminated end of the specimen (see Fig. 5). One edge of the specimens was then painted white with a brittle Enamel paint and marked at 5 mm intervals to enable crack length to be monitored during the test. Crosshead speeds of 0.01 mm/min and 0.05 mm/min were used during the loading and unloading cycles, respectively. The load and the ram displacement were recorded on a computer throughout the test, including the unloading cycle.

4. Four-point bend testing of CIA: results

4.1. Single-step (VARTM) CIA beams

The load–deflection curves of the four SS-SC15 CIA beams, for which the rubber layer was mechanically prepared, are shown in Fig. 6 wherein it is observed that the reproducibility in strength is very good. The coefficients of variation for the first visually observed failure load and displacement were about 8%. In Fig. 6, the load–displacement response of the CIA beams is seen to be non-linear, with maximum displacements recorded of about 50–70 mm, which are several times the thickness of the beams. Large deformation, material non-linearity and damage progression are therefore important in the structural response of the beams. The events leading to the progressive deterioration of the structural performance of the specimens were nevertheless observed to be similar for all the SS-SC15 beams, and they are described next.

For clarity, the load–displacement curve of the SS-SC15_1 specimen is reproduced in Fig. 7. The load–displacement curve of the CIA is linear for displacement below about 2 mm. After 2 mm displacement a gradual change in the stiffness of the beams is observed. At a displacement of 7 mm, and a load of 7.5 kN, a ‘kink’ in the load–displacement curve may be clearly observed. This ‘kink’ corresponds to a drastic change in the stiffness of the beams. The non-linear response of the beams may be though to be associated with the yielding and damage of the resin at the resin-filled gaps between two tiles. Indeed, Huang et al. [10] have shown that stress concentrations existed at that location as a result of the discontinuities of the tiles. The non-linear deformation of the resin will in-turn progressively reduce the stiffness of the beam. This effect is later confirmed by the analysis of the strain gauge readings.

After 7 mm displacement, the load increases steadily, although with a lower stiffness, until a first fracture event is seen to occur consistently at an average displacement and load of 23.7 mm and 14.9 kN, respectively. This drop in stiffness was accompanied by a noticeably audible cracking

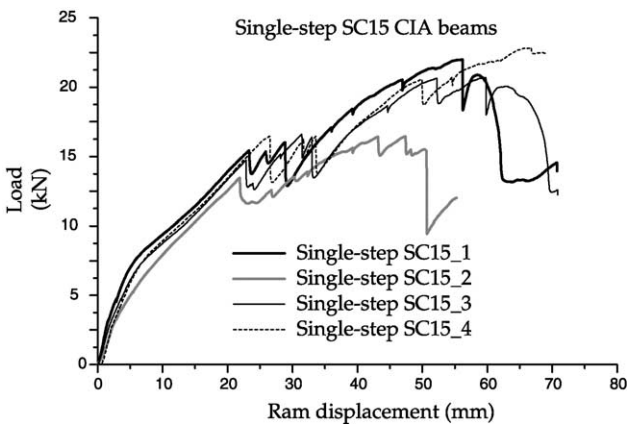

Fig. 6. Load–deflection responses of SS-SC15 (VARTM) CIA beams.

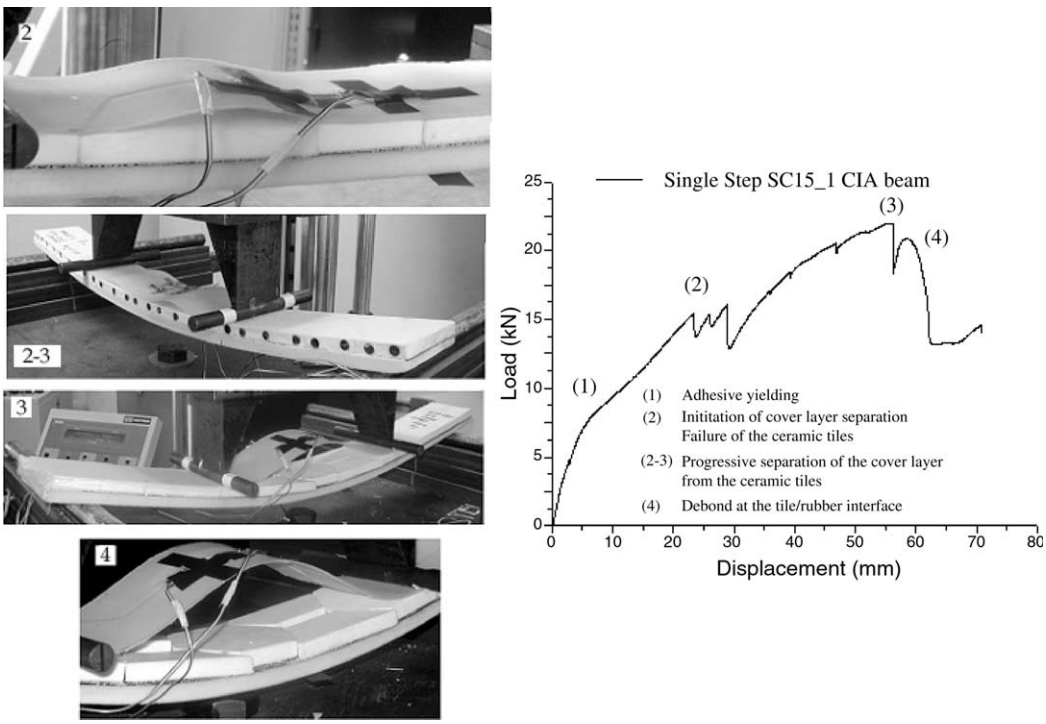

Fig. 7. Sequence of failure events of SS-SC15 CIA beams.

noise and was due to the sudden release of strain energy that appeared to have resulted from the separation of the cover layer from the ceramic tiles, as shown in Fig. 7(2). The separation of the cover layer was observed to initiate at the edge of the beams, and in a symmetric fashion. The locus of failure was interfacial.

The observation of the edges of the beams at that instant during the tests also revealed the formation of discrete tensile cracks in some ceramic tiles. The exact sequence of event was, however, not observable. The cracking also resulted from the process of stress transfer between the cover layer and the ceramic tiles, as shown schematically in Fig. 8. Stress transfers from the cover layer to the ceramic tile, through the resin interlayer, in a shear lag process originating at the resin-filled gaps between the tiles [10]. This shear lag process progressively increases the contribution of the ceramic tiles to the structural stiffening, resulting in high axial stresses being developed that could generate cracks in the ceramic.

The next sequence of failure event was observed to be the progressive separation of the cover layer from the ceramic tiles, as the displacement is increased above 24 mm, as shown in Fig. 7(2) and (3). The delamination progressed from the edge toward the center of the beams, and from the center half-tiles toward the center full-tile. The initiation and the propagation of the separation of the cover layer form the ceramic tiles was a repeatable event and it may be possible to improve the strength of the CIA beams by

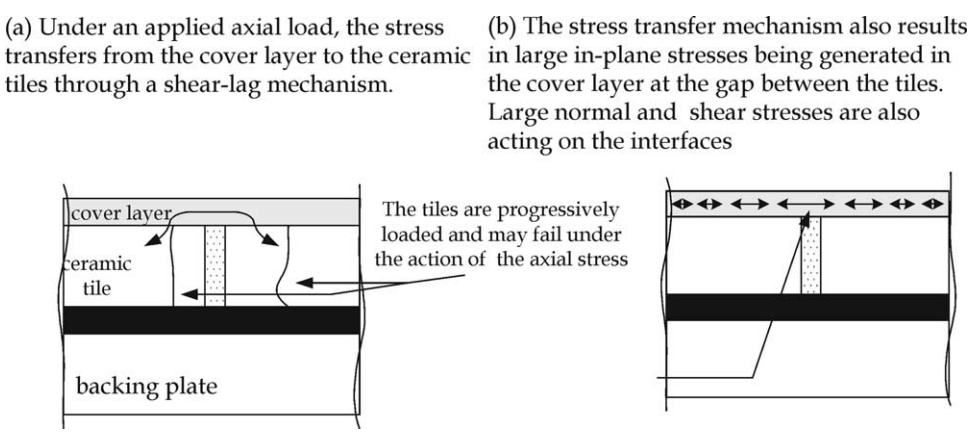

Fig. 8. Mechanism of stress transfer between the cover layer and the ceramic tiles.

improving the adhesion level between the cover layer and the ceramic tiles. For instance, it has been shown that a silane-coupling agent could improve the strength of alumina ceramic to vinyl-ester lap joints [23]. It is noted that such failure event may be as a consequence of the specimen geometry and the anticlastic effect imposed by the bending test. Nonetheless, it is still useful information, and clearly indicates that the interface strength between the tiles and the cover layer is weak. This information may be valuable, since cover layers are prone to barely visible impact damages, which causes small delaminations that may propagate and lead to unstable fracture under load. The cover layer may be seen completely debonded from the ceramic tiles in Fig. 7(3). This event was observed to occur at the maximum load, in average 18.7 kN.

The collapse of the specimens corresponded to the separation of the ceramic tiles from the rubber layer, Fig. 7(4). The tests were stopped after this event has occurred. This collapse event may be seen to result from the juxtaposition of material layers with different stiffness. Indeed, under the action of a pure bending moment, the backing plate, isolated from the stiff tiles by the rubber layer, may curve as a beam in simple bending would. However, the stiff and thick ceramic tiles remain flat and undistorted. One of the functions of the rubber layer is therefore to uncouple the backing plate from the ceramic tiles, allowing the structure to deform under load. It may then be seen that there is a limit to which the independent bending of the layers is possible. Indeed, the ceramic tiles, by remaining undistorted, try to peel away from the backing plate and the rubber layer, and the ultimate strength of the structure is therefore dependent on the adhesion strength between the rubber layer and the ceramic tiles.

The evolution of the axial surface strains with load are shown in Fig. 9 for three out of the four SS-SC15 beams tested. The strains at the centerlines of the backing plate (SG3), the cover layer (SG1) and at the resin-filled gap between two tiles on the cover layer (SG2) were recorded. The reproducibility in recorded strains is very good, with the data from the three specimens overlapping each other.

In Fig. 9, the axial strains on the surface of the backing plate, SG3, are tensile and reflect the progression of the damages discussed earlier. The strains on the backing plate may be seen to increase until a load of about 15 kN, after which the separation of the cover layer from the ceramic tiles progressively degrades the structural performance of the CIA beam. The cover layer separation decouples the ceramic tiles from the structure, hence limiting their participation in the load bearing.

In Fig. 9, the strains recorded on the cover layer, SG1, may be seen to be largely unaffected by the separation of the cover layer from the ceramic tiles. Also in Fig. 9, the strains measured over the resin-filled gap between two tiles, SG2, are much greater than the strains measured at the center of the full-size tile. A strain concentration of about six may be observed for a load below 6 kN. This may be seen to arise due to the mechanism of stress transfer form the cover layer to the ceramic tile, as was shown schematically in Fig. 8. As we move away from the edges of the tiles, and the stress transfers from the cover layer to the tile, the strains in the cover layer decreases to a far-field value, and the ceramic tiles are effectively loaded. The resulting stress was earlier shown to result in the cracking of the tiles. The cover layer strains are therefore a minimum at a distance away from the gap between two tiles (that distance depends on the thickness and stiffness of the adhesive interlayer [10]), but maximum at the gap between two tiles, as indicated in Fig. 9.

Also, it is noted that the SG2 strains increase linearly up to a load of about 7 kN, after which the trace may be seen to deviate, as a result of yielding or damage occurring in the resin. It may be recalled that a ‘kink’ in the load–displacement response of the CIA occurred at a load of about 7.5 kN. The departure of linearity of the strain reading may be seen to correspond to the large drop in the stiffness of the beams. The progressive yielding and damage of the adhesive may hence explain the progressive reduction in the stiffness of the beams observed in the load–displacement curves.

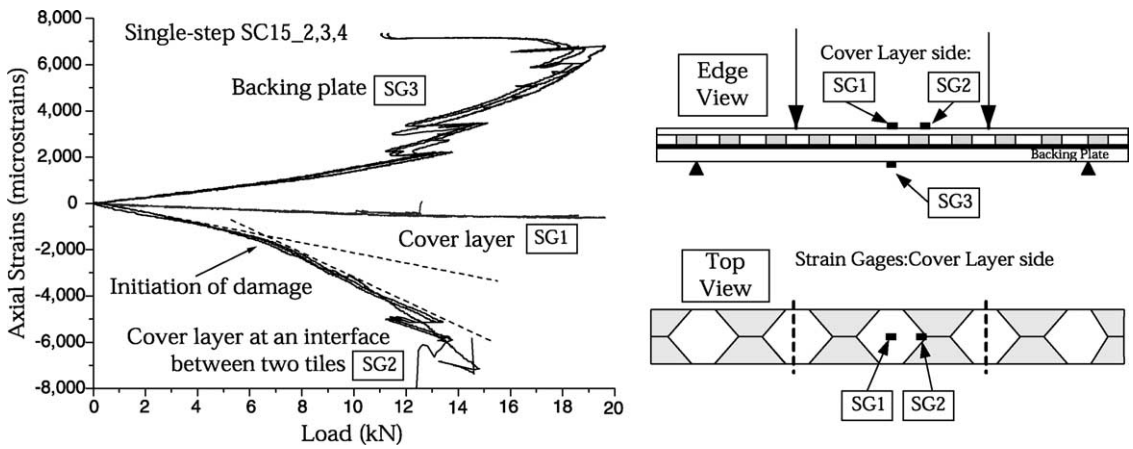

Fig. 9. Evolution of axial strains with load.

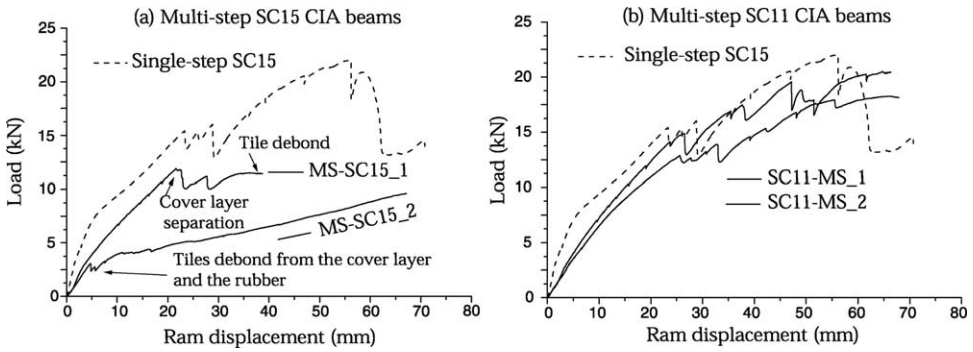

Fig. 10. Load–deflection responses of MS-SC15 and MS-SC11 CIA beams.

4.2. Multi-step CIA beams

Load–deflection curves of the multi-step and single-step beams are shown in Fig. 10. In Fig. 10(a), the load–deflection responses of the two multi-step SC15 (MS-SC15) beams tested may be compared with that of a representative SS-SC15 beam. The structural responses of the two MS-SC15 beams tested are quite different from each other. The MS-SC15_2 beam failed at a low load by the separation of the ceramic tiles from both the cover layer and the rubber layer. This premature failure is thought to be as a result of an improper surface preparation of the rubber layer (such as contaminant left on the surface), for which the exact causes were not identified in the present work. In comparison, the MS-SC15_1 beam was found to be much stronger, but not as strong as the single-step specimens. The initiation of failure of the MS-SC15_1 beam was observed to be by the separation of the cover layer from the ceramic tiles, as for the single-step beams, but at a lower load of 11.7 kN (i.e. compared with 14.9 kN for the single-step manufactured beams). The ultimate collapse of the beams occured prematurely by the separation of the ceramic tiles from the rubber layer. This represents a 20% drop in strength. Consequently, the structural performance of the MS-SC15 specimens may be seen to be poorer than that of the SS-SC15 specimens. Furthermore, the initial stiffness of the beam (i.e. for displacement lower than 20 mm) was seen to be lower than that of the single-step manufactured beam; about 50% lower. This will be shown to be a result of the larger spacing between the tiles that results from the multi-step fabrication process.

The load–deflection response of the two multi-step SC11 (MS-SC11) CIA beams tested is compared with that of a SS-SC15 beam in Fig. 10(b). The scatter is relatively small. The structural performance of the MS-SC11 beams compares well with that of a SS-SC15 beam, although their initial stiffness is lower. Also, the progressive degradation of the MS-SC11 beams was observed to be comparable with that of the SS-SC15 beams.

4.3. Effect of the surface mechanical preparation of the rubber layer

In Fig. 11, the structural responses of single- and multi-step manufactured beams, for which the rubber layer was and was not mechanically abraded, are compared. It is observed that the mechanical abrasion of the rubber layer has a critical effect on the structural performance of the CIA beams. In Fig. 11(a), the lack of abrasion leads to a reduction in failure displacement and load of about 75 and

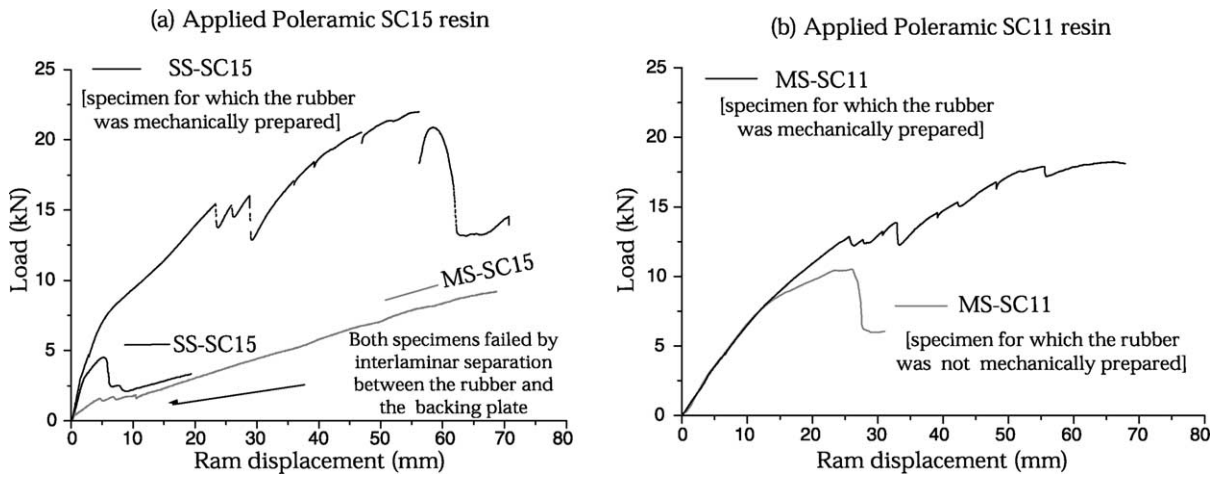

Fig. 11. Load–deflection responses of single- and multi-step (a) SC15 and (b) SC11 CIA beams. Effect of the mechanical roughening of the rubber.

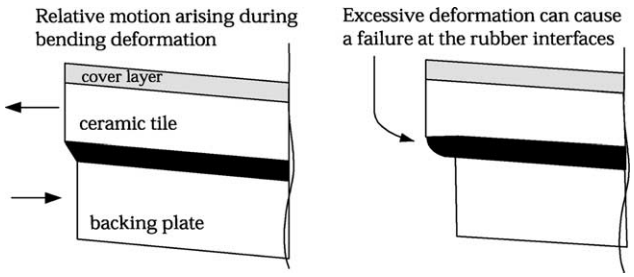

Fig. 12. Relative motion between the backing plate and the upper layer of the CIA.

85% for the single-step and the MS-SC15 specimens. In Fig. 11(b), the mechanical performance of MS-SC11 beams for which the rubber layer was and was not mechanically prepared are compared. Again, it may be seen that the mechanical performance is poorer for the specimen for which the rubber layer was not mechanically prepared. These beams failed by the separation of the rubber from the backing plate, as a result of a poorer level of adhesion between the two constituents, as shown schematically in Fig. 12. Consequently, it may be seen that the surface mechanical preparation of the rubber layer is necessary to achieve optimum mechanical performance of the beams.

5. Four-point bend testing of CIA: discussion

In Fig. 10, it was observed that the manufacturing process and the resin system have a large effect on the structural performance of the beams. The structural performance of SS-SC15 beams was seen to be superior to any of the CIA beams tested in the present work. The structural performance of the MS-SC15 beams was comparatively seen to be the poorest of all the CIA beams, as a result of a premature decohesion of the ceramic tiles from the rubber layer. In contrast, the structural performance of the MS-SC11 beam was seen to be comparable, although with a lower initial stiffness, to that of the single-step manufactured beams.

In Fig. 13, the observation of the cross-sectional areas (spanning the width) of a single-step and a multi-step CIA beam reveals that the gap spacing two tiles is in average 0.5 and 1.5 mm for the single-step and the multi-step CIA beams, respectively. The difference in the confinement of the tiles can be traced back to the manufacturing processes. In the single-step process, the resin is infused, in one operation, through the sections of the beam. As a result, the tiles may be uniformly spaced and compacted. On the other hand, in the multi-step process the backing plate, already manufactured and cut to dimension, is solid and prevents the tiles to be as well compacted. As a result, the gap in between two tiles is seen to vary from tile to tile, and is generally greater than for the single-step CIA beams. A larger gap spacing results in a more compliant response of the multi-step beams. At the gap between two tiles, it was shown that the stress transfers in a shear-lag process, giving rise to the high strain concentrations observed in Fig. 9. For small gap spacing, the stress transfer efficiency is high [24], therefore maximizing the participation of the stiff ceramic tiles to the structural stiffness of the CIA. Increasing the gap spacing decrease the efficiency of the shear-lag process, resulting in a loss in initial structural stiffness, since the contribution of the stiff ceramic tile to the structural stiffness is diminished; multi-step beams are more compliant than single-step beams.

Furthermore, it is startling that the single-step and the MS-SC15 beams behave in different ways. Consider that in the single-step process, the backing plate and the rubber layer are bonded together at the same time as the CIA is impregnated; the material layers are bonded at the same time as the backing plate is made. A SC15 resin rich interlayer is formed at the interface between the backing plate and the rubber layer. It is reminded that a 0.1 mm thick scrim cloth was inserted during manufacturing at that location to ensure a constant interlayer thickness. As a result, the transition between the backing plate and the rubber layers may be thought to be smooth, with only one interphase region forming close to the rubber layer, as shown in Fig. 14(a). However, in the multi-step process, Fig. 14(b) and (c), a cured backing plate is bonded to the rubber layer. The interlayer resin rich zone, similar to an adhesive interlayer in a bonded joint, may be seen to give rise to two interphase regions, one above and one below the interlayer resin rich zone. The interphase regions in the multi-step manufactured beam may therefore be seen to be weaker than for a single-step manufactured beams.

6. Effect of the manufacturing process on the level of adhesion at the interface between the rubber layer and the backing plate

The effect of the fabrication method on the level of adhesion achieved between the backing plate and the rubber

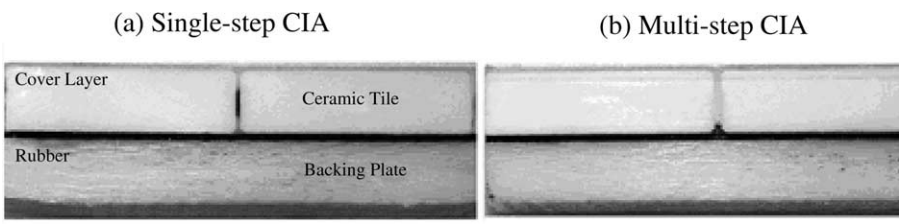

Fig. 13. Single- and multi-step manufactured specimens.

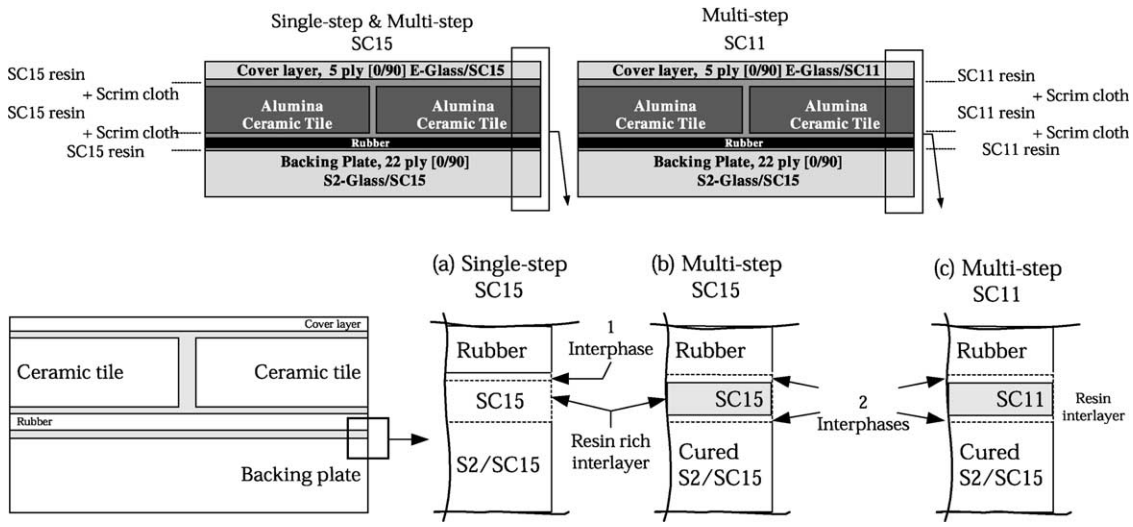

Fig. 14. SS-SC15 and MS-SC15 and SC11 CIA beams.

layer is examined using DCB specimens, as was shown in Fig. 5. Five DCB specimens were prepared for each manufacturing process (SS-SC15, MS-SC15 and MS-SC11).

Several data reduction methods were assessed; namely the corrected beam theory (CBT) [25], the experimental compliance [26], and the area [25] methods. In the CBT approach, the strain energy release rate, G, may be calculated from knowledge of the load and the opening displacement of the arms and the measured crack length (measured from the center of the loading blocks to the crack tip with a traveling microscope), with a data reduction technique presented in Ref. [25]. The experimental compliance method (ECM) uses experimental data to compute the value of fracture toughness, and the data reduction technique used is described in Ref. [26]. The specimens were not pre-cracked, and the initiation and propagation values were determined in one loading/unloading cycle. The area method involves the measurement of the loading/unloading curves for successive increments of crack length [25]. The strain energy release rates were calculated from two consecutive loading lines, corrected for zero displacement at zero loads.

Three specimens were used for the determination of G by the compliance method and two specimens were used for the determination of G by the area method. Fig. 15 shows the calculated Mode I fracture toughness for single-step manufactured specimens. It may be noted that the values calculated from the CBT and the ECM approaches agree very well, and agree with the values calculated from the area method.

Fracture toughness data, calculated with the CBT approach, for the single-step and multi-step DCB specimens are listed in Table 2. The value given in Table 2 is an average of the propagation values (i.e. not taking into consideration the initiation values). The loci of failure are also given. It may be noted that the rising R-curves (i.e. the resistance to crack propagation, G, increases with crack length, a), as shown in Fig. 15, do not permit the calculation of a single value for the fracture toughness of the specimens. The values given in Table 2 are therefore only an indication that may be use for a comparison of the results. Also, it was not possible to assess the fracture toughness of the DCB specimens bonded with the SC11 resin system. The load–displacement curves of the MS-SC11 DCB specimens were found to be highly non-linear. Furthermore, the onset of crack growth was not well defined, and it was not possible to note accurately the crack length, as required by the data reduction method. Consequently, it was not possible to calculate a value of fracture toughness. Consequently, only the DCB specimens bonded with SC15 resin system are analyzed in the present paper.

In Table 2, the manufacturing process may be seen to have a significant effect on the values of Mode I fracture toughness. For the specimens with the rubber layer mechanically prepared, it may be seen that the single-step DCB specimens were the toughest, with a toughness of

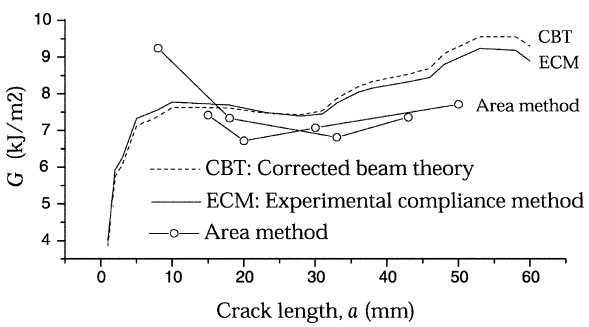

Fig. 15. Comparison between the fracture toughness values calculated by the CBT [25], ECM [26] and area [25] approaches for the single-step manufactured DCB.

Table 2
Fracture toughness of the representative DCB specimens

Specimens	G (J/m^2)	Locus of failure
SS-SC15	6700	Cohesive (rubber)
MS-SC15	1500	Cohesive/interfacial
MS-SC15[a]	400	Interfacial

[a] The rubber layer was not mechanically prepared.

about 6700 J/m^2 on average. The single-step DCB specimens were further seen to fail cohesively within the rubber layer, and the crack path was located roughly about 3/4 of the thickness of the rubber layer. The high fracture toughness is attributed to crack blunting and local strain strengthening mechanisms that increase the apparent value of fracture toughness. Such mechanisms were observed to occur at the crack tip as the crack propagated, e.g. fibrils were seen to span the blunted crack faces, as shown in Fig. 16. Such mechanisms may furthermore be thought to be responsible for the rising R-curves observed in Fig. 15.

In Table 2, the fracture toughness for the multi-step DCB specimens with mechanically prepared rubber layers is about 75% lower than that of the corresponding single-step DCB specimens. The locus of failure was mixed, i.e. cohesive and interfacial. The drop in fracture toughness is unexpected as there is no important difference in the processing conditions between the single-step and the multi-step processes; the SC15 resin system hardens at room temperature. The drop in fracture toughness of the multi-step specimens may be explained by considering the interface conditions produced by the single-step and the multi-step processes, as discussed previously for the CIA beams and as shown in Fig. 14. In the single-step process, a resin rich layer between the backing plate and the rubber layer is created as part of the backing plate material, i.e. only one interphase exists at the backing plate/rubber interface (Fig. 14(a)). However, in the multi-step process, the SC15 resin system is used as an 'adhesive' to join the already cured backing plate and the rubber layer. Therefore, two interphases exist (Fig. 14(b) and (c)). One at the interface between the backing plate/resin interlayer and the other at the resin interlayer/rubber. The SC15 resin, however, is not a structural adhesive, and, provided that the rubber is appropriately prepared, the backing plate/resin interlayer may be the weak link, promoting the interfacial/cohesive fracture observed in the multi-step specimens.

Furthermore, in Table 2, with no mechanical treatment of the rubber, the fracture toughness of the multi-step DCB specimens may be seen to be the lowest. The intephase between backing plate and rubber may now be seen to be very weak which leads to a premature failure of the specimens. The locus of failure for these specimens was purely interfacial. The mechanical treatment of the rubber layer provided an increase in surface area as well as an increase in chemical reactivity of the surface, which, as a result, provided an increased level of intrinsic adhesion.

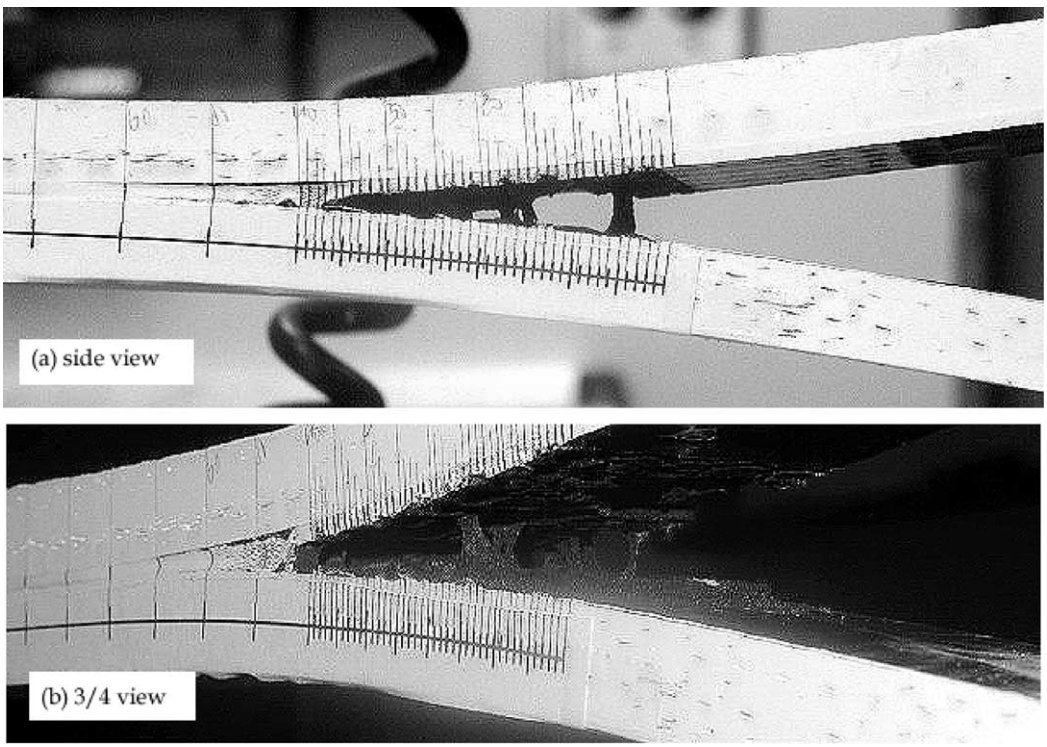

Fig. 16. Details of the fracture of SS-SC15 DCB specimens.

Overall, the behavior of the single-step and multi-step DCB coupons may be seen to be comparable with that of the CIA beams.

7. Conclusions

Beams, representative of CIA, were tested in four-point bending and have been shown to be able to support loads far exceeding the load associated with the initial failure event. The structural performance of the beams has been shown to degrade progressively with increasing displacement. The structures were shown to provide significant load capacity and toughness before final collapse occurred. The structural performance of a CIA beam has also been related to its manufacturing process. CIA beams fabricated from a single-step VARTM process outperformed beams manufactured by a more conventional multi-step process. This is encouraging since single-step manufacturing methods are more efficient.

The structural performance of the beams was furthermore seen to be dependent on the performance of the interfaces that compose the beams. Firstly, the surface preparation of the rubber layer was seen to be essential for the structural performance of the CIA beams. Secondly, the adhesion between the rubber and the backing plate on one hand, and the ceramic tiles on the other, was also seen to be critical. Consequently, an increase in the mechanical performance of the CIA beams may be achieved by the tailoring of the strength of its interfaces. Hence, there is a need to develop test coupons, representative of the different interfaces present in the CIA beams, which can be used to evaluate the performance of the interfaces.

DCB specimens, representative for the backing plate/rubber interface of single-step and multi-step CIA beams were tested. Coupons representative for the single-step VARTM CIA beams failed by crack propagation in the rubber layer (cohesive fracture of the rubber). On the other hand, the coupons representative of the multi-step CIA beams failed at the interface, although some rubber cohesive failure zones were observed. The mechanical roughening of the rubber layer also resulted in an improvement in the adhesion between the GFRP and the rubber. The behavior of the single-step and multi-step DCB coupons was comparable to that of the CIA beams.

Acknowledgements

The authors would like to acknowledge funding from the Army Research Laboratory as part of the Strategic Environmental Research and Development Program (SERDP) (Grant DAAL01-98-K-0058) and the Composite Materials Technology Center of Excellence program established at the University of Delaware Center for Composite Materials.

References

[1] Gama BA, Bogetti TA, Fink BK, Yu CJ, Claar TD, Eifert HH, Gillespie Jr. JW. Aluminum foam integral armor: a new dimension in armor design. Compos Struct 2001;52:381–95.

[2] Gama BA, Gillespie JW, Bogetti TA, Fink BK. Innovative design and ballistic performance of lightweight composite integral armor. Technology for the army's transformation. SAE World Congress and Exposition, Detroit; March 5–8, 2001. Paper No. 2001-01-0888.

[3] Mahfuz H, Zhu Y, Haque A, Abutalib A, Vaidya U, Jeelani S, Gama B, Gillespie JW, Fink BK. Investigation of high-velocity impact on integral armor using finite element method. Int J Impact Engng 2000; 24(2):203–17.

[4] Gama BA, Gillespie JW, Mahfuz H, Bogetti TA, Fink BK. Effect of non-linear material behavior on the through-thickness stress wave propagation in multi-layer hybrid lightweight armor. In: Atluri SN, Burst FW, editors. International Conference on Computational Engineering and Sciences, 21–25 August 2000, vol. I. Los Angeles, CA: Tech Science Press; 2000. p. 157–62.

[5] Heider D, Graf A, Fink BK, Gillespie JW. Feedback control of the vacuum assisted resin transfer molding (VARTM) process. Proceedings of the SPIE International Symposium on NDE Techniques for Aging Infrastructure and Manufacturing: Process Control and Sensors for Manufacturing; 1999.

[6] Kerang H, Shunliang J, Chuck Z, Wang B. Flow modeling and simulation of SCRIMP for composites manufacturing. Composites, Part A 2000;31(1):79–86.

[7] Gama BA, Li H, Li W, Paesano A, Heider D, Gillespie JW. Improvement of dimensional tolerances during VARTM processing. Proceedings of 33rd International SAMPE Technical Conference, Nov 5–8 2001; 2001. p. 1415–27.

[8] Fink BK, McKnight SH, Gillespie JW. Co-injection resin transfer molding for optimization of integral armor. Proceedings of the 21st Army Science Conference: Science and Technology for Army After Next, Norfolk, VA; June 15–17, 1998.

[9] Pike T, McArthur M, Schade D. Vacuum assisted resin transfer molding of a layered structural laminate for application on ground combat vehicles. Int SAMPE Tech Conf 1996;28(Nov):374–80.

[10] Huang XG, Gillespie JW, Kumar V, Gavin L. Mechanics of integral armor: discontinuous ceramic-cored sandwich structure under tension and shear. Compos Struct 1996;36:81–90.

[11] Monib AM, Gillespie JW. Damage tolerance of composite laminates subjected to ballistic impact. Proceedings of ANTEC 98, Brookfield, CT: Society of Plastics Engineers; 1998. p. 1463–7.

[12] DeLuca E, Prifti J, Betheney W, Chou SC. Ballistic impact damage of S2-glass reinforced plastic structural armor. Compos Sci Technol 1998;58(9):1453–61.

[13] Sherman D. Impact failure mechanisms in alumina tiles on finite thickness support and the effect of confinement. Int J Impact Engng 2000;24(3):313–28.

[14] Camacho GT, Ortiz M. Computational modeling of impact damage in brittle materials. Int J Solids Struct 1996;33(20–22): 2899–938.

[15] Martinez MA, Chocron IS, Rodriguez J, Sanchez Galvez V, Sastre LA. Confined compression of elastic adhesives at high rates of strain. Int J Adhes Adhes 1998;18(6):375–83.

[16] Zaera R, Sanchez-Saez S, Perez-Castellanos JL, Navarro C. Modeling of the adhesive layer in mixed ceramic/metal armors subjected to impact. Composites, Part A 2000;31:823–33.

[17] Chocron Benloulo IS, Sánchez-Gálvez V. A new analytical model to simulate impact onto ceramic/composite armors. Int J Impact Engng 1998;21(6):461–71.

[18] Fellows NA, Barton PC. Development of impact model for ceramic-faced semi-infinite armour. Int J Impact Engng 1999; 22(8):793–811.

[19] Davila CG, Chen T-K. Advanced modeling strategies for the analysis of tile-reinforced composite armor. Appl Compos Mater 2000;7(1): 51–68.
[20] Davila CG, Smith C, Lumban-Tobing F. Analysis of thick sandwich shells with embedded ceramic tiles. NASA TM-110278 1996;12.
[21] Chen T-K, Davila CG, Baker DJ. Analysis of tile-reinforced composite armor. Part 2. Viscoelastic response modeling. Proceedings of the 21st Army Science Conference, Science and Technology for Army After Next, Norfolk, VA; June 1998.
[22] Davila CG, Chen T-K, Baker DJ. Analysis of tile-reinforced composite armor. Part 1. Advanced modeling and strength analyses. Proceedings of the 21st Army Science Conference, Science and Technology for Army After Next, Norfolk, VA; June 1998.
[23] Tanoglu M, McKnight SH, Palmese GR, Gillespie JW. Use of silane coupling agents to enhance the performance of adhesively bonded alumina to resin hybrid composites. Int J Adhes Adhes 1998;18:431–4.
[24] Mahdi S, Gillespie JW. Finite element analysis of multi-functional tile-reinforced sandwich constructions. Sent for review in Composites Part B:Engineering, 2003.
[25] Hashemi S, Kinloch AJ, Williams JG. The analysis of interlaminar fracture in uniaxial fibre-polymer composites. Proc R Soc Lond 1990; A427:173–99.
[26] ASTM D 5528-94a, Standard test method for Mode I interlaminar fracture toughness of unidirectional fiber-reinforced polymer matrix composites. Annual book of ASTM standards, vol. 15.03. USA: ASTM; 1997.